Multi-scale structure of the electron diffusion region

H. Karimabadi,[1] W. Daughton,[2] and J. Scudder[2]

Received 7 April 2007; revised 8 May 2007; accepted 6 June 2007; published 11 July 2007.

[1] Kinetic simulations of magnetic reconnection indicate that the electron diffusion region (EDR) can elongate into a highly stretched current layer with a width on the electron scale and a length that exceeds tens of ion inertial lengths. The resulting structure has no fluid analogue and consists of two regions in the exhaust direction. The inner region is characterized by the locale where electrons reach a peak outflow speed near the electron Alfvén velocity. Ions also approach ~80% of their peak velocity in this inner region but remain sub-Alfvénic. There exists a large electrostatic potential that can temporarily trap electrons within this inner region. The electron frozen-in condition is violated over a wider outer region characterized by highly collimated electron jets that are gradually decelerated and thermalized. Reconnection proceeds continuously but the rate is modulated in time as the EDR elongates into an extended layer. The elongation of the EDR is controlled by the competition between the outward convection of magnetic flux and the non-ideal term involving the divergence of the electron pressure tensor. The occasional balance between these two terms leads to periods of quasi-steady reconnection. However, over longer time scales, a natural feature of the reconnection process appears to be frequent formation of plasmoids due to the instability of the elongated EDR which leads to larger variations in the reconnection rate. These new findings provide testable predictions and indicate the need to reconsider the diagnostics for identification of the diffusion region and interpretation of observational data.
Citation: Karimabadi, H., W. Daughton, and J. Scudder (2007), Multi-scale structure of the electron diffusion region, *Geophys. Res. Lett.*, *34*, L13104, doi:10.1029/2007GL030306.

1. Introduction

[2] The basic structure and role of the electron diffusion region (EDR) in magnetic reconnection are the subject of recent controversy. While it is generally agreed that the onset of reconnection is controlled by the details of electron physics, the view articulated in the GEM challenge and related studies has been that the subsequent nonlinear evolution of the system and the resulting reconnection rate are controlled by the ions [e.g., *Birn et al.*, 2001; *Shay et al.*, 2001; *Rogers et al.*, 2001]. According to these models, the EDR remains stable and is localized on the electron scale in both the inflow and outflow directions. In this scenario, the non-ideal electron region extends $\sim 5d_e$ in the outflow direction while the ion diffusion region extends $\sim 10d_i$, where d_e and d_i are the electron and ion inertial lengths. However, recent simulations have brought these results into question [*Daughton et al.*, 2006; *Fujimoto*, 2006]. Using large-scale fully kinetic simulations with both periodic and open boundary conditions, the structure of the EDR was observed to elongate in time along the exhaust direction with scales $\sim 5-20d_i$ while maintaining an electron scale thickness in the inflow direction [*Daughton et al.*, 2006].

[3] In this work, the structure of the EDR is examined in detail using new diagnostics to objectively quantify the spatial region in which the electrons are demagnetized. The results indicate that the EDR consists of two distinct regions in the exhaust direction. The inner layer is characterized by a strong out-of-plane electron current that is produced by the reconnection electric field. This electron flow is turned into the outflow direction by the Lorentz force leading to an intense in-plane current layer or "outflow jet". These electron jets are found to extend to $\pm 10d_i$ before they are decelerated and thermalized. We demonstrate that the elongation of the EDR is a natural consequence of the rapid outward convection of magnetic flux due to the electron outflow jets. Reconnection proceeds continuously but the rate is modulated in time due to the elongation of the EDR. The expansion is counteracted by a localizing effect arising from the divergence of the electron pressure tensor and this leads to occasional periods of quasi-steady reconnection during which variations in the rate are relatively small. However, over longer time scales the elongated electron layers are unstable to plasmoid formation leading to larger variations in the rate. These findings are at odds with previous theoretical expectations and require rethinking of data analysis for existing missions as well as planning of the upcoming Magnetospheric Multiscale mission. One of the clear predictions of this work is the presence of thin but highly elongated, non-gyrotropic electron jets associated with the reconnection site.

2. Simulation Setup and Parameters

[4] We consider a Harris equilibrium with zero guide field using a coordinate system where the initial magnetic field is $B_x = B_o \tanh(z/L)$, where L is the half-width of the layer. The density profile is $n(z) = n_o \mathrm{sech}^2(z/L) + n_b$ where n_o is the peak Harris density and n_b is the background density. Results are presented from two fully kinetic simulations with open boundary conditions [*Daughton et al.*, 2006] and larger system sizes than considered previously. The first case (run 1) is $50d_i \times 50d_i$ where d_i is an ion inertial length based on n_o. The simulation parameters are $L/d_i = 0.91$, $m_i/m_e = 100$, $T_i/T_e = 5$, $n_b/n_o = 0.3$, $\omega_{pe}/\Omega_{ce} = 3$, 2560×2560 cells with 3×10^9 particles. The second case (run 2) has a larger system size $100d_i \times 100d_i$ with parameters $L/d_i = 0.35$, $T_i = T_e$, $\omega_{pe}/\Omega_{ce} = 2$, 2048×2048 cells with 2.5×10^9 particles and other parameters the same as run 1.

[1]Department of Electrical and Computer Engineering, University of California, San Diego, La Jolla, California, USA.
[2]Department of Physics and Astronomy, University of Iowa, Iowa City, Iowa, USA.

0094-8276/07/2007GL030306$05.00

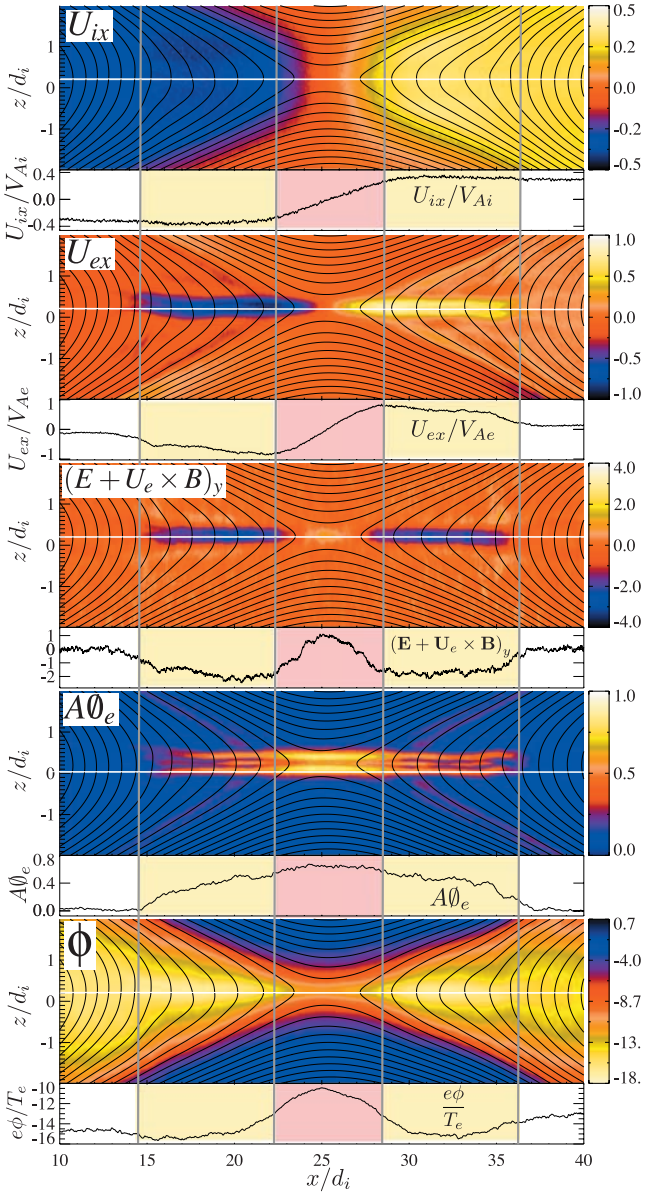

Figure 1. Results from run 1 at $t\Omega_{ci} = 80$ showing ion outflow U_{ix}, electron outflow U_{ex}, non-ideal electric field $(\mathbf{E} + \mathbf{U}_e \times \mathbf{B})_y$ (normalized by E_y at x-point), electron agyrotropy $A\emptyset_e$ and electrostatic potential normalized to the initial electron temperature $e\phi/T_e$. Black lines correspond to flux surfaces and 1D line plots are along the horizontal white line indicated in each panel.

Both simulations employ a weak long wavelength perturbation [*Daughton et al.*, 2006].

3. Multi-Scale Structure

[5] The structure of the reconnection layer is shown in Figure 1 at $t\Omega_{ci} = 80$ for run 1. In the first two panels, the ion and electron outflow velocities are normalized by their respective Alfvén speed $V_{As} = B_s/(4\pi m_s n_b)^{1/2}$ based on the magnetic field upstream of the ion and electron diffusion regions ($B_i \approx 0.78\ B_o$ for ions and $B_e \approx 0.36\ B_o$ for electrons). The non-ideal electric field $(\mathbf{E} + \mathbf{U}_e \times \mathbf{B})_y$ is shown in the third panel, followed by the electron agyrotropy $A\emptyset_e \equiv 2|P_{\perp e1} - P_{\perp e2}|/(P_{\perp e1} + P_{\perp e2})$ which ranges from a maximum of 2 down to 0 in the gyrotropic limit. Nonzero $A\emptyset_e$ indicates demagnetization of thermal electrons. In the last panel, the electrostatic potential ϕ is normalized by the initial uniform electron temperature T_e. Below each quantity is a 1D cut along the horizontal line indicated. Figure 1 reveals interesting features as well as a number of surprises.

[6] The 1D cuts clearly show the multi-scale nature of the EDR. The length D_e of the inner region is defined by the location where the electrons reach their peak outflow velocity (shaded red). The ions going through this layer are also accelerated over a similar scale to ~80% of their peak velocity. The acceleration of ions within this region is due to the presence of the electrostatic potential. In contrast, the electrons are accelerated by the reconnection electric field E_y and redirected into the outflow by the Lorentz force. Notice that the electrostatic potential acts to counteract this turning process and thus may play a key role in determining the structure of the layer. The length Δ_e of the outer region is identified by the location where the electrons become fully magnetized $A\emptyset_e \rightarrow 0$, marked by the vertical lines. This occurs much farther out and coincides with the termination of the electron jets. The electron bulk flow slows down in the outer layer, converted partially to thermal energy. In most of the inner layer the electrons lag the field $(\mathbf{E} + \mathbf{U}_e \times \mathbf{B})_y > 0$ whereas in the outer layer $(\mathbf{E} + \mathbf{U}_e \times \mathbf{B})_y < 0$ indicating that electrons are outrunning the field. The electron pressure tensor balances this non-ideal electric field in the vicinity of the x-point and continues to play a dominant role along the entire length of the EDR.

[7] The full length of the electron jets are seen to extend to $\Delta_e \sim 20d_i$ in the exhaust direction rather than the expected $10d_e$ [e.g., *Shay et al.*, 2001]. In the previous studies, the location of the peak electron outflow velocity was argued to be where the electrons start to become fully magnetized. In the present study, the elongation of D_e to ion scales drives an intense electron outflow jet that forces the point of full magnetization Δ_e farther downstream, giving rise to a two-scale structure in the outflow direction.

[8] The electron outflow velocity is near the theoretical limit of the electron Alfvén velocity $U_{ex} \approx V_{Ae}$ based on conditions upstream of the EDR. This is not sufficient to overcome the bottleneck that arises from the elongation of D_e, and thus variations in the reconnection rate are observed.

[9] The ion outflow velocity is significantly less than the Alfvén speed $U_{ix} \approx 0.4V_{Ai}$ using the proper normalization based on upstream conditions. This is considerably below the expected value based on the traditional understanding [e.g., *Shay et al.*, 1999]. This may be partly due to the presence of significant pressure gradients in these solutions.

[10] There exists a large in-plane electrostatic field associated with the inner layer and also along the separatrices. The potential difference between the x-point and the edge of the inner layer (red region) is nearly $e\phi/T_e \sim 4$ in Figure 1. This implies that most electrons are temporarily trapped within the inner region until they gain enough energy from the reconnection electric field to escape. This process may

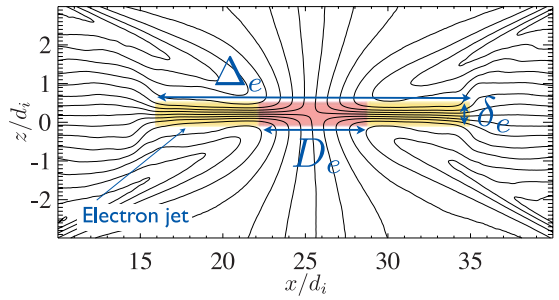

Figure 2. The multi-scale structure of electron diffusion region. The black lines are the electron streamlines for run 1 at $t\Omega_{ci} = 80$. The inner region (red) corresponds to nearly uniform electron inflow and strong out-of-plane current while the yellow regions correspond to the extended electron outflow jets.

play a crucial role in determining the structure and energy exchange within the layer.

[11] From these results, we have developed a new picture of the EDR as illustrated in Figure 2. The resulting electron layer has a width on the order $\delta_e \sim 2 - 4d_e$ and a total length that can exceed $\Delta_e > 20d_i$ in the exhaust direction. The inner portion of the EDR centered about the x-point (shaded red) corresponds to a nearly uniform inflow as indicated by the electron streamlines. The length D_e of this region coincides with the location where electrons reach their maximum outflow speed near V_{Ae}. Beyond the inner region, the electron jets start to slow down whereas ions continue to accelerate. The outer edge of EDR is defined by the location where electrons become magnetized as determined by the abrupt drop in the agyrotropy $A\emptyset_e$ as shown in Figure 1. This also corresponds to the termination of the electron jet and where the frozen-in condition is again satisfied $\mathbf{E} + \mathbf{U}_e \times \mathbf{B} \approx 0$. These results point to a more complex structure of the electron diffusion region than previously expected. In the traditional picture, the length of the non-ideal region is well marked by the region of inflowing plasma. In contrast, the new results indicate a significant inflow of electrons only in the inner region while strong deviations from the frozen-in condition persist to much larger distances exceeding $10d_i$.

4. Physical Mechanism for the Elongation

[12] We start with the generalized Ohm's law

$$\mathbf{E} + \frac{\mathbf{U}_e \times \mathbf{B}}{c} = -\left[\frac{1}{en_e}\nabla \cdot \mathbf{P}_e + \frac{m_e}{e}\frac{d\mathbf{U}_e}{dt}\right] \equiv \mathbf{G}, \qquad (1)$$

where $\mathbf{G}$ denotes the non-ideal terms. Combining this equation with Faraday's law along the centerline of the outflow ($z = 0$) yields:

$$\frac{\partial B_z}{\partial t} = -c\frac{\partial E_y}{\partial x} \approx -\frac{\partial}{\partial x}\left(U_{ex}B_z + cG_y\right). \qquad (2)$$

The first term on the right-hand side is the convective term that in the frozen-in limit expresses the outward convection of magnetic flux (e.g., due to electron jets). Since the profiles of U_{ex} and B_z are both antisymmetric about the x-point, the product must be of the form $U_{ex}\,B_z \propto x^2$ for some region about the x-point. Simulations indicate this corresponds approximately to the shaded red region in Figures 1 and 2. In the limit $G_y \rightarrow 0$, the convection term alone implies $\partial|B_z|/\partial t < 0$ within this region, indicating a collapse of the 2D structure into an elongated 1D current layer. Clearly at the x-point, a finite G_y is required to balance the reconnection electric field E_y. However, the non-ideal terms also must play an essential role in determining the length of the layer. While it has been argued that Hall physics gives rise to a constant $U_{ex}\,B_z$ in the outflow direction [*Rogers et al.*, 2001], this clearly does not apply within the EDR. Instead, the dynamical evolution of the inner region (red in Figures 1–2) is controlled by the competition between the outward convection $U_{ex}\,B_z$ which elongates the layer and the localizing influence of G_y.

[13] In the outer region (yellow in Figures 1 and 2) the convection term $U_{ex}\,B_z$ is a decreasing function of x as the electron outflow jets slow down. The deceleration of the jets is accompanied by a large increase in electron pressure (factor of 7 increase between the x-point and the end of jet in Figure 1) which may partially regulate the length Δ_e. However, to achieve a steady-state balance for this region the non-ideal terms in (2) are again essential.

[14] These arguments imply that the expansion of the EDR will continue unless it can be balanced by the second term and/or interrupted by some other dynamic process such as the formation of a secondary island which can interrupt the expansion by forming two competing x-points [*Daughton et al.*, 2006; *Daughton and Karimabadi*, 2007].

[15] To determine which terms dominate the balance in (2), Figure 3 shows the cut along the outflow of E_y, $U_{ex}B_z$, and the two terms comprising G_y, namely, dU_{ey}/dt and $(\nabla \cdot \mathbf{P}_e)_y$ at three different times for run 1. The spatial profile of G_y provides a measure of the region where the frozen-in condition is broken and is dominated by $(\nabla \cdot \mathbf{P}_e)_y$ at most locations along the outflow. It is useful to draw a parallel to fluid models and think of the spatial extent of G_y as the region of finite "effective resistivity", even though the physics of $\nabla \cdot \mathbf{P}_e$ is very different than classical resistivity. It is apparent from Figure 3 that the mechanism that breaks the frozen-in condition is spatially localized, with significant gradients in the inner region, and with both its magnitude and spatial extent changing in time. At $t\Omega_{ci} = 42$, the two terms on the right hand side of (2), $U_{ex}B_z$ and G_y, are clearly out of balance, with G_y more localized than $U_{ex}B_z$ indicating the EDR is still expanding. At $t\Omega_{ci} \sim 48$, a secondary island forms which leads to a temporary halt in the elongation. Between $t\Omega_{ci} = 70-120$, however, the $U_{ex}B_z$ term is nearly balanced by the non-ideal terms giving rise to a uniform E_y. During this interval, both the structure of the EDR and the observed reconnection rate are nearly stationary. However, the total length $\Delta_e \approx 20d_i$ is comparable to what previous researchers had predicted for the ion diffusion region!

5. Time Dependence of Reconnection

[16] A clear correlation between the elongation of the inner region D_e and the reconnection rate was demonstrated by *Daughton et al.* [2006]. The elongation of D_e, if

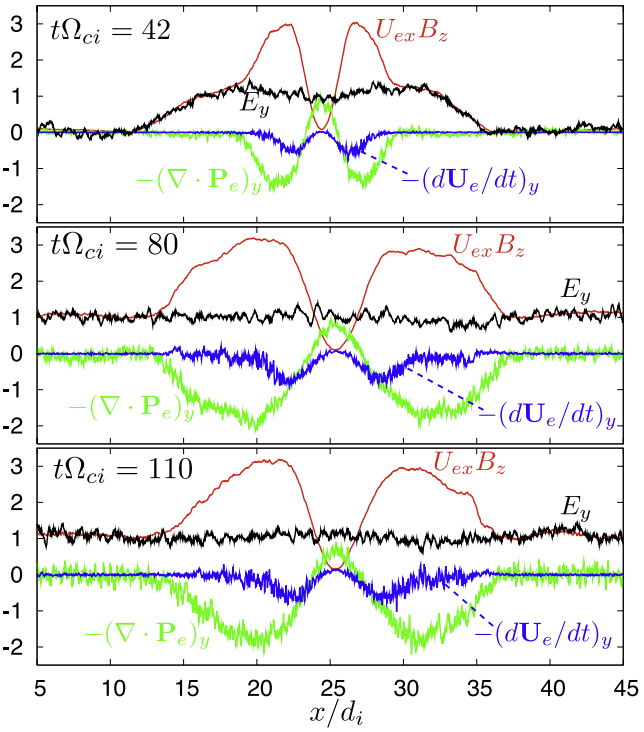

Figure 3. Various terms in (1) along outflow $z = 0$ for run 1 at three selected time slices. Terms in each panel are time averaged over an interval $\Delta t\Omega_{ci} = 2$ and then normalized by the electric field E_y at time $t\Omega_{ci} = 80$.

continued unchecked, would lead to a significant reduction of the reconnection rate. However, as demonstrated in Figure 3, the divergence of the electron pressure tensor can at times balance the convection term and temporarily halt the expansion of the EDR. This leads to quasi-steady behavior of the reconnection rate over some time interval.

[17] The normalized reconnection rate is computed from

$$E_R \equiv \frac{c}{B_i V_{Ai}} \langle E_y \rangle \tag{3}$$

where $\langle E_y \rangle$ denotes the average electric field at the x-point over a time interval $2\Omega_{ci}^{-1}$ and both B_i and V_{Ai} are evaluated upstream of the ion diffusion region (at $z \approx 2.5d_i$). In the presence of multiple x-points, this expression is evaluated for each and the maximum rate is selected. Figure 4 shows time evolution of E_R for runs 1 and 2. The peak rate is the same for both cases followed by a decrease in time as D_e elongates. Both runs show periods of quasi-steady E_R during which the terms in (2) approximately balance. The larger system (run 2) transitions into the continual formation of secondary islands for $t\Omega_{ci} > 90$ leading to larger variations in the reconnection rate. This suggests that reconnection may be inherently unsteady in large-scale systems.

6. Conclusions

[18] Our results indicate that the electron diffusion region (EDR) forms a highly elongated layer with multiple-scales and a structure that is very different than previous expectations. The scale of the inner region of the EDR is in the range $D_e \approx 7-11d_i$ for the two simulations considered with mass ratio $m_i/m_e = 100$. A more recent simulation with parameters similar to run 2 but with $m_i/m_e = 400$ resulted in $D_e \sim 6.5$ versus $9d_i$ for run 2 measured at the same time $t\Omega_{ci} = 50$. This is consistent with the weak mass ratio scaling of $D_e/d_i \sim (m_e/m_i)^{1/4}$ first reported by *Daughton et al.* [2006]. For the physical mass ratio of hydrogen, this implies a scale of $D_e \sim 3 - 5d_i$ for the inner region of the EDR, but more work is needed to accurately determine the scaling with electron mass and temperature. The outer region of the EDR is longer and more dynamic with scales as large as $\Delta_e \sim 20d_i$ in run 1 and $\Delta_e \sim 40d_i$ in run 2. Thus even at realistic mass ratio it is expected that Δ_e may extend to tens of d_i.

[19] These findings have important consequences for identification of the EDR and interpretation of observational data for both existing and upcoming missions. For example, the full length of the non-ideal electron region would be a factor of 40–100 larger than previous estimates. One clear prediction that may be observationally testable is the presence of a thin ($\delta_e \sim 4d_e$) super-Alfvénic agyrotropic electron jet that may extend large distances from the x-line.

[20] The dynamical evolution of the EDR is controlled by a competition between the outward convection of magnetic flux and the localizing effect of $\nabla \cdot \mathbf{P}_e$. These two processes can balance at times, giving rise to a quasi-steady reconnection rate, although the system as whole remains time-dependent. One of the controversial issues regarding reconnection at the magnetopause has been whether reconnection occurs in a continuous or intermittent (switching on and off) fashion. Our results indicate that the number and location of x-lines can change in time but there always remains at least one x-line in the system and the macroscopic reconnection rate remains continuous but with modulations in time. This appears consistent with a recent Cluster study by *Phan et al.* [2004]. In the present simulations, the duration of quasi-steady reconnection is $\sim 50\Omega_{ci}^{-1}$ corresponding to ~15 seconds at the magnetopause, but longer durations cannot be ruled out. One natural feature of the reconnection process appears to be the frequent formation of plasmoids resulting from the instability of the elongated EDR. This may have relevance

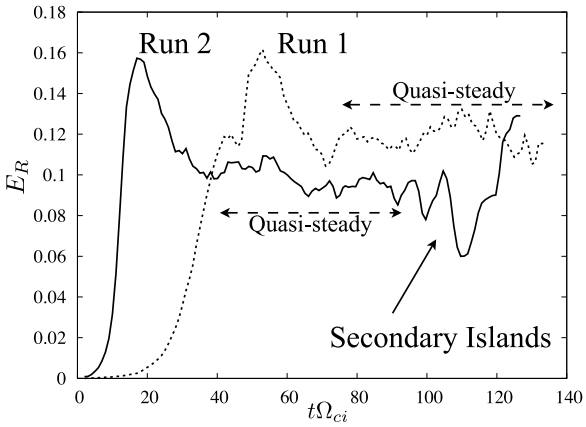

Figure 4. Reconnection rate normalized to conditions upstream of the ion diffusion region for run 1 (dashed line) and run 2 (solid line).

to observations of plasmoids in the magnetotail and flux transfer events (FTEs) in the dayside magnetopause.

[21] Finally, these results are based entirely on 2D simulations which do not permit instabilities in the out-of-plane direction such as the lower-hybrid drift mode. The influence of these instabilities on the structure of the reconnection layer remains an open question.

[22] **Acknowledgments.** This work was supported by NASA grants NNG05GJ25G, NNG05GJ01G, and IGPP grant, NSF grant 0447423, and by the DOE under award DE-FG02-06ER54893. Simulations were partially performed at LANL.

References

Birn, J., et al. (2001), Geospace Environmental Modeling (GEM) Magnetic Reconnection Challenge, *J. Geophys. Res.*, *106*(A3), 3715–3719.

Daughton, W., and H. Karimabadi (2007), Collisionless magnetic reconnection in large-scale electron positron plasmas, *Phys. Plasmas*, in press.

Daughton, W., J. Scudder, and H. Karimabadi (2006), Fully kinetic simulations of undriven magnetic reconnection with open boundary conditions, *Phys. Plasmas*, *13*(7), 072101.

Fujimoto, K. (2006), Time evolution of the electron diffusion region and the reconnection rate in fully kinetic and large system, *Phys. Plasmas*, *13*(7), 072904.

Phan, T. D., et al. (2004), Cluster observations of continuous reconnection at the magnetopause under steady interplanetary magnetic field conditions, *Ann. Geophys.*, *22*, 2355–2367.

Rogers, B. N., R. E. Denton, J. F. Drake, and M. A. Shay (2001), Role of dispersive waves in collisionless magnetic reconnection, *Phys. Rev. Lett.*, *87*, 195004.

Shay, M. A., J. F. Drake, B. N. Rogers, and R. E. Denton (1999), The scaling of collisionless, magnetic reconnection for large systems, *Geophys. Res. Lett.*, *26*(14), 2163–2166.

Shay, M. A., J. F. Drake, M. B. N. Rogers, and R. E. Denton (2001), Alfvénic collisionless magnetic reconnection and the Hall term, *J. Geophys. Res.*, *106*(A3), 3759–3772.

W. Daughton and J. Scudder, Department of Physics and Astronomy, University of Iowa, Iowa City, IA 52242, USA.

H. Karimabadi, Department of Electrical and Computer Engineering, University of California, San Diego, 9500 Gilman Drive, La Jolla, CA 92093-0407, USA. (homa@ece.ucsd.edu)